

# Doppler-free spectroscopy of the $^1S_0$ – $^3P_0$ optical clock transition in laser-cooled fermionic isotopes of neutral mercury

M. Petersen, R. Chicireanu, S.T. Dawkins, D.V. Magalhães,\*

C. Mandache,† Y. Lecoq, A. Clairon, and S. Bize

*LNE-SYRTE, Observatoire de Paris*

*75014 Paris, France.*

(Dated: February 10, 2022)

## Abstract

We have performed for the first time direct laser spectroscopy of the  $^1S_0$ – $^3P_0$  optical clock transition at 265.6 nm in fermionic isotopes of neutral mercury laser-cooled in a magneto-optical trap. Spectroscopy is performed by measuring the depletion of the magneto-optical trap induced by the excitation of the long-lived  $^3P_0$  state by a probe at 265.6 nm. Measurements resolve the Doppler-free recoil doublet allowing for a determination of the transition frequency to an uncertainty well below the Doppler-broadened linewidth. We have performed absolute measurement of the frequency with respect to an ultra-stable reference monitored by LNE-SYRTE fountain primary frequency standards using a femtosecond laser frequency comb. The measured frequency is  $112857529080 \pm 5.6$  kHz in  $^{199}\text{Hg}$  and  $1128569561140 \pm 5.3$  kHz in  $^{201}\text{Hg}$ , more than 4 orders of magnitude better than previous indirect determinations. Owing to a low sensitivity to blackbody radiation, mercury is a promising candidate for reaching the ultimate performance of optical lattice clocks.

---

\*Also at Instituto de Física de São Carlos, USP-PO Box 369, 13560-970, São Carlos, SP, Brazil.

†Also at National Institute for Laser Physics, Plasmas and Radiation, Plasmas and Nuclear Fusion Laboratory, Bucharest, Magurele, PO Box MG 7, Romania.

The performance of optical atomic clocks is improving at a high pace. Optical clocks are now surpassing atomic fountain clocks based on microwave transitions [1, 2, 3, 4]. Some of these optical transitions are now recognized as secondary representations of the unit of time of the international system of units (SI) opening the way to a new definition of the SI second based on an optical transition in the coming years. Atomic clocks also represents a powerful tool for testing fundamental physical laws. For instance, stability of natural constants and thereby that of fundamental interactions (electro-weak, strong interaction) can be tested to high levels of precision, providing constraints that are independent of any assumption related to cosmological models [1, 5, 6, 7, 8, 9]. Such tests provide precious experimental information to help the search for unified theories of fundamental interactions.

Optical lattice clocks using strontium atoms have now demonstrated accuracies at the  $10^{-16}$  level [3], a factor of  $\sim 4$  better than the best atomic fountains but still a factor of  $\sim 4$  worse than the best optical single ion clock based on  $\text{Al}^+$  [1]. At this level of uncertainty, the blackbody radiation shift is the largest correction and the largest contribution to the strontium clock uncertainty. In future development, the blackbody radiation shift will remain a severe limitation to the accuracy at the  $10^{-17}$  level. An optical clock using ytterbium [10] will have the same limitation since the blackbody shift is no more than a factor of 2 smaller in fractional terms [11]. In contrast, neutral mercury has been recognized as having a low sensitivity to blackbody radiation [12, 13, 14] whilst retaining all other desirable features for an optical lattice clock. Mercury has the potential to achieve uncertainty in the low  $10^{-18}$  and therefore to compete with the best single ion optical clocks [1]. Mercury is also an interesting candidate in the search for variations of natural constants owing to its relatively high sensitivity to variations of the fine structure constant [15]. However, laser cooling of neutral mercury has been pursued and achieved only recently [14, 16] due to the challenging requirement of deep-UV laser sources.

In this paper, we report the first direct laser spectroscopy of the  $^1S_0$ – $^3P_0$  clock transition at 265.6 nm in the two naturally occurring fermionic isotopes of mercury. Spectroscopy is performed on a sample of cold atoms released from a magneto-optical trap (MOT). We this approach, we resolve the Doppler-free recoil doublet allowing for a determination of the transition frequency with an uncertainty well under the Doppler-broadened linewidth. Absolute measurement of the frequency is performed using an optical frequency comb.

Figure 1 shows the low-lying energy levels of mercury. Mercury has an alkaline-earth

like electronic structure similar to those of strontium or ytterbium. In our experiment, laser cooling of mercury is achieved using the  $^1S_0-^3P_1$  transition at 253.7 nm with a natural linewidth of 1.3 MHz. Cooling light is provided by quadrupling a Yb:YAG thin disk laser delivering up to 7 W of single frequency light at 1014.8 nm. A commercially available doubling stage using a temperature tuned LBO crystal within a bow-tie configuration build-up cavity generates up to 3 W of power at 507.4 nm. A second doubling stage uses a 90°-cut anti-reflection coated 7 mm long angle tuned BBO, also in a bow-tie configuration. Out-coupling of the second harmonic at 253.7 nm is achieved by using an harmonic separator mirror as one of the build-up cavity mirrors. Up to 800 mW of CW power have been generated with this system. In practice, the system is set to generate 100 to 150 mW to avoid the rapid degradation of the harmonic separator observed at higher output power. The frequency of this light is stabilized to the saturated absorption feature observed in a room temperature mercury vapor cell with a 1 mm interaction length. The residual jitter is estimated to be less than 100 kHz which is suitably small compared to the 1.3 MHz natural linewidth of the cooling transition.

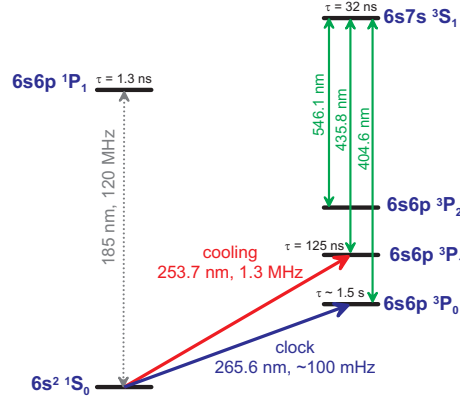


FIG. 1: Relevant energy levels of mercury. The  $^1S_0 - ^3P_1$  transition at 253.7 nm is used for magneto-optical trapping. The clock transition studied in this paper is the  $^1S_0 - ^3P_0$  transition at 265.6 nm. The mentioned natural linewidth of  $\sim 100$  mHz is for  $^{199}\text{Hg}$  based on [17].

A 2 dimensional magneto-optical trap (2D-MOT) geometry [18] is used to generate a slow atom beam which in turn is used to load a conventional MOT. A vapor pressure of  $\sim 2 \times 10^{-7}$  mbar of mercury is kept in the 2D-MOT chamber by cooling a few grams of mercury held in a copper bowl down to  $-55^\circ\text{C}$  using two stage Peltier element inside the vacuum chamber. The 2D-MOT is formed at the intersection of two orthogonal pairs of

$\sigma^+ - \sigma^-$  polarized retro-reflected beams with a total power of  $\sim 50$  mW. The longitudinal and transverse diameters at  $1/e^2$  are  $\sim 10$  mm and  $\sim 8$  mm. The intersection overlaps with the center of a 2-dimensional quadrupole magnetic field with a gradient of  $0.2 \text{ mT.mm}^{-1}$  generated by 4 rectangularly shaped coils located outside the vacuum chamber. A 1.5 mm diameter and 10 mm long hole in the 2D-MOT chamber allows the beam of slow atoms confined at the center of the quadrupole field through, while providing high differential pumping between the 2D-MOT and the MOT chambers. The slow atom beam is directed toward the center of the MOT, 70 mm away from the output of the 2D-MOT. The MOT is generated at the intersection of three orthogonal pairs of retro-reflected  $\sigma^+ - \sigma^-$  polarized laser beams with a diameter of  $\sim 6.6$  mm and a power of  $\sim 15$  mW each. Coils located outside the vacuum chamber generate the magnetic quadrupole field with a gradient of  $0.15 \text{ mT.mm}^{-1}$  along the strong axis. Our present setup forces the detuning of the 2D-MOT and the MOT to be the same. We find that a red detuning of  $-5.5$  MHz corresponding to  $-4.4 \Gamma$  optimizes the number of atoms in the MOT. Detection of the MOT is performed by collecting fluorescence light onto a low noise photodiode. Measurements with the most abundant  $^{202}\text{Hg}$  isotope indicate that  $\sim 5 \times 10^6$  atoms are captured with a loading time constant of 2.3 s. Further measurements of atom number based on absorption of a weak 253.7 nm probe are in agreement.  $^{199}\text{Hg}$  and  $^{201}\text{Hg}$  isotopes typically show slightly reduced atom numbers.

As shown in fig. 2, laser light at 265.6 nm for probing the  $^1S_0 - ^3P_0$  clock transition is generated by frequency quadrupling the 1062.5 nm output of a distributed feedback (DFB) laser diode delivering 250 mW of useful light. The first doubling is accomplished with 64% efficiency using a periodically-poled KTP crystal and a bow-tie build-up cavity, leading to 160 mW at 531.2 nm. The second doubling uses an angle-tuned  $90^\circ$ -cut anti-reflection coated BBO crystal and delivers up to 7 mW at 265.6 nm. The DFB laser diode is injection-locked to an ultra-stable laser source. As shown in fig. 2, this laser source is composed of a Yb-doped DFB fiber laser stabilized to an ultra-stable Fabry-Pérot cavity. A fraction of the light is sent through an actively phase-stabilized fiber link to stabilize an optical frequency comb generated by a Ti:Sa femtosecond laser whose repetition rate is measured against the LNE-SYRTE flywheel oscillator [19], which is monitored by several primary fountain frequency standards. Repeated measurements of the ultra-stable laser source have shown highly predictable behavior, relaxing the need for simultaneous operation of the optical

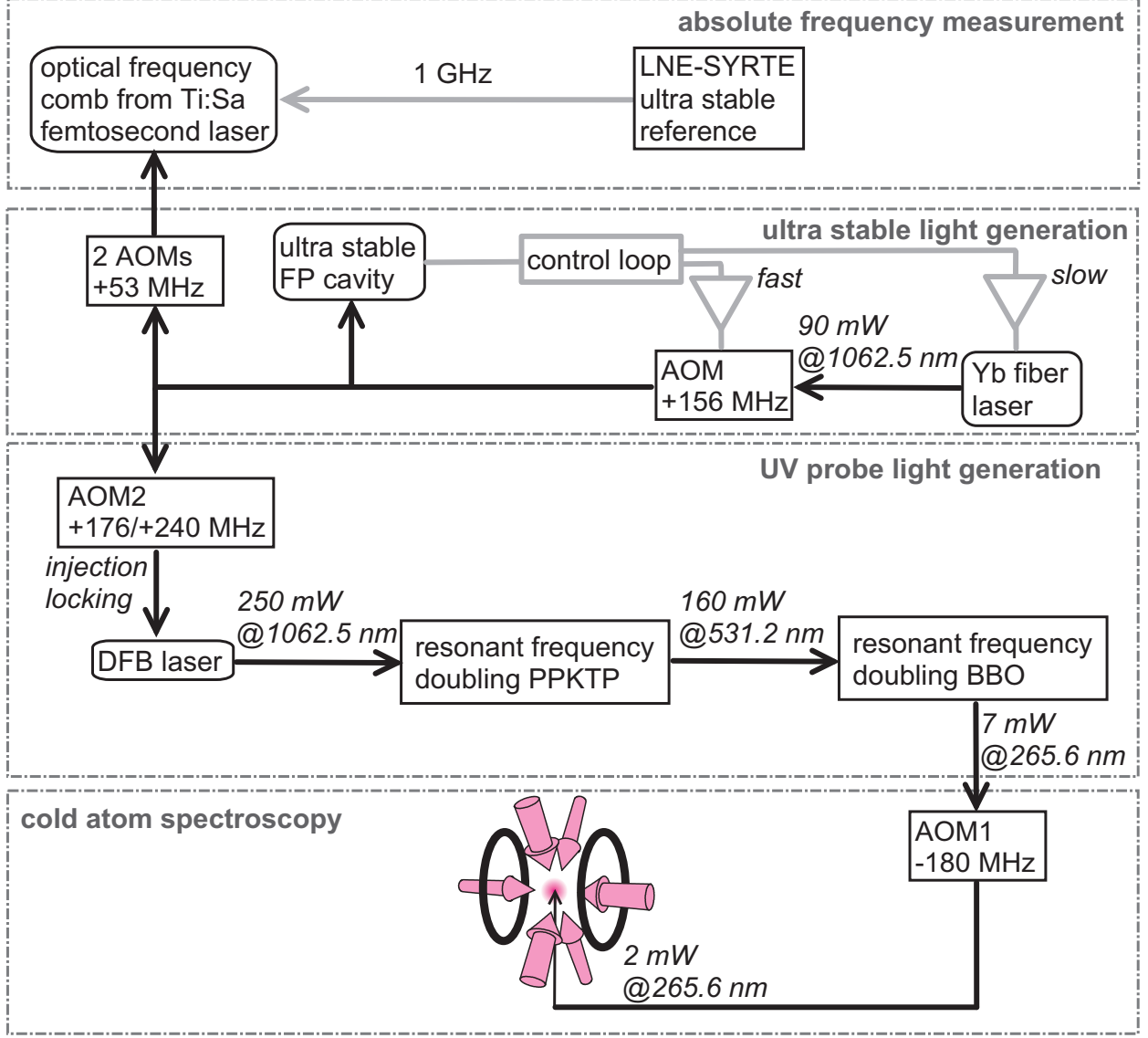


FIG. 2: Generation of the probe light at 265.6 nm and referencing to primary frequency reference. AOM2 frequency depends on the isotope.

frequency comb with the rest of the experiment at the current level of accuracy. Typically, measurements against the primary frequency reference were performed several times a day which is sufficient to estimate the optical frequency to better than 100 Hz at 1062.5 nm or 4 parts in  $10^{13}$ . Although this is adequate for the present work, it is noteworthy that this probe laser system already has the capability of highly stable and accurate referencing limited only by primary frequency standards. In fact, during the initial search for the clock transition, the Yb-doped fiber laser was stabilized to a component of the optical frequency comb, itself locked to the primary reference with a controllable offset to allow for broader

scanning of the probe laser.

Spectroscopy of the clock transition is performed according to the scheme proposed and demonstrated with strontium [20] and further used with ytterbium [21]. An up-going probe beam crosses the MOT at its center and is either retro-reflected or not. Initially, the search for the clock transition was performed with both the MOT and the probe beam on continuously. Fluorescence of the MOT was monitored as a function of the probe frequency. Excitation of atoms in the untrapped, long-lived  $^3P_0$  state excited by the probe laser and their subsequent fall under gravity induces losses in the MOT. Up to 90% depletion of the MOT has been observed. To suppress the light shift of  $\sim 300$  kHz induced by the 253.7 nm MOT beams and perform accurate measurements, the following scheme is implemented. Using a mechanical shutter, the 2D-MOT and MOT beams are switched on for an adjustable duration of 20 to 50 ms then off for 5 ms. During the 5 ms, the probe light is pulsed once with adjustable delay and duration using acousto-optical modulator AOM1 in fig. 2. This cycle is repeated continuously. During the 5 ms, the atomic cloud is freely falling over  $122\ \mu\text{m}$  and expanding by  $180\ \mu\text{m}$  at the Doppler temperature of  $31\ \mu\text{K}$ . Atoms are therefore recaptured when the MOT is turned back on. The MOT reaches a steady state determined by the loading rate during the MOT on time and the losses induced by the excitation of the  $^3P_0$  state. Average fluorescence of the MOT is measured while stepping the probe frequency using AOM2 in fig. 2.

Measurements were first taken with a  $1.4 \times 0.24$  mm up-going probe beam. The maximum depletion of the MOT is  $\sim 50\%$ . The observed peak is Doppler-broadened to a linewidth ranging from 360 kHz to 550 kHz full-width at half maximum, depending on the MOT parameters including the quality of beam alignment. The lowest observed linewidth corresponds to a temperature of  $36\ \mu\text{K}$ , which is close to the Doppler temperature of  $31\ \mu\text{K}$  related to the natural linewidth of the cooling transition. Further measurements were performed with a retro-reflected probe beam in order to cancel the Doppler shift which is due to acceleration of the atoms under gravity and to a possible non-vanishing average velocity of the cloud released from the MOT. Comparisons of the frequency with single passed and retro-reflected beams first led to estimating the uncertainty related to the Doppler effect at  $\sim 30 - 40$  kHz. Further optimization of the retro-reflected geometry (size and overlap of the returning beam) allowed for the observation of the Doppler-free features expected for a retro-reflected probe. Figure 3 shows a  $^{199}\text{Hg}$  spectrum measured with a probe diameter

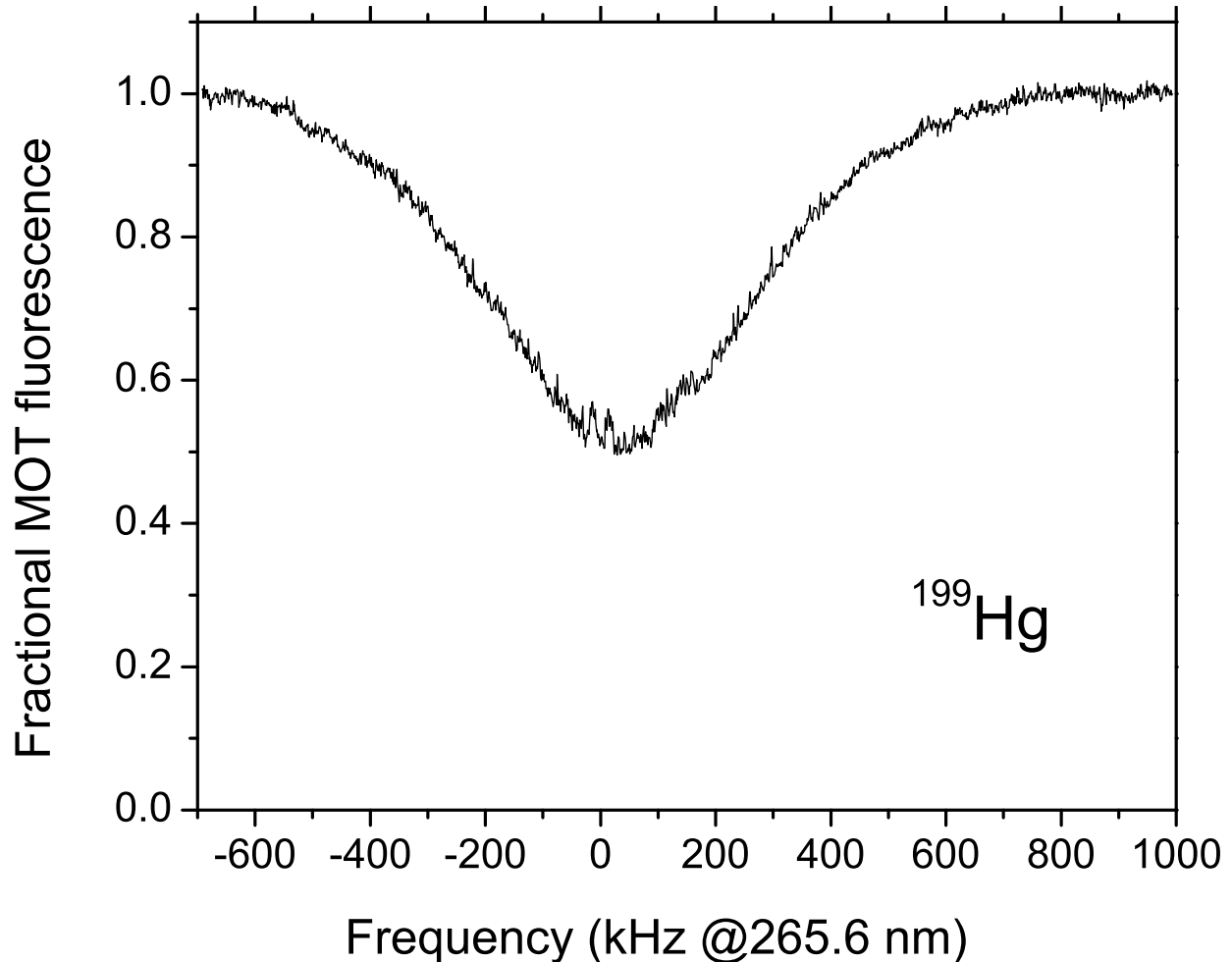


FIG. 3: Spectrum of  $^1S_0 - ^3P_0$  transition in  $^{199}\text{Hg}$  observed with a retro-reflected probe beam. Sharp Doppler-free features can be seen at the top of the 580 kHz wide Doppler profile.

of  $280\text{ }\mu\text{m}$  at  $1/e^2$  and the maximum available power of 2 mW. Two sharp features can be distinguished at the top of the Doppler profile which is 580 kHz wide in this example.

The two features, which are better seen on the narrower scans of fig. 4, are the Doppler-free recoil doublet [22]. The recoil features are shifted by  $\pm\nu_{\text{recoil}}$  with respect to the atomic transition frequency  $\nu$ , where  $\nu_{\text{recoil}}$  is the recoil frequency of the transition equal to  $\nu \times (h\nu/2mc^2)$  or 14.2 kHz, where  $c$  is the speed of light,  $h$  is Planck's constant and  $m$  is the atomic mass. The measured splitting matches  $2\nu_{\text{recoil}}$  within the overall statistical error bar of  $\lesssim 1\text{ kHz}$ . We have also checked that the center of each component of the recoil doublet is unchanged to less than 1 kHz when the probe time is changed by a factor of 2. Instead, under our experimental conditions, the width of the recoil components is proportional to

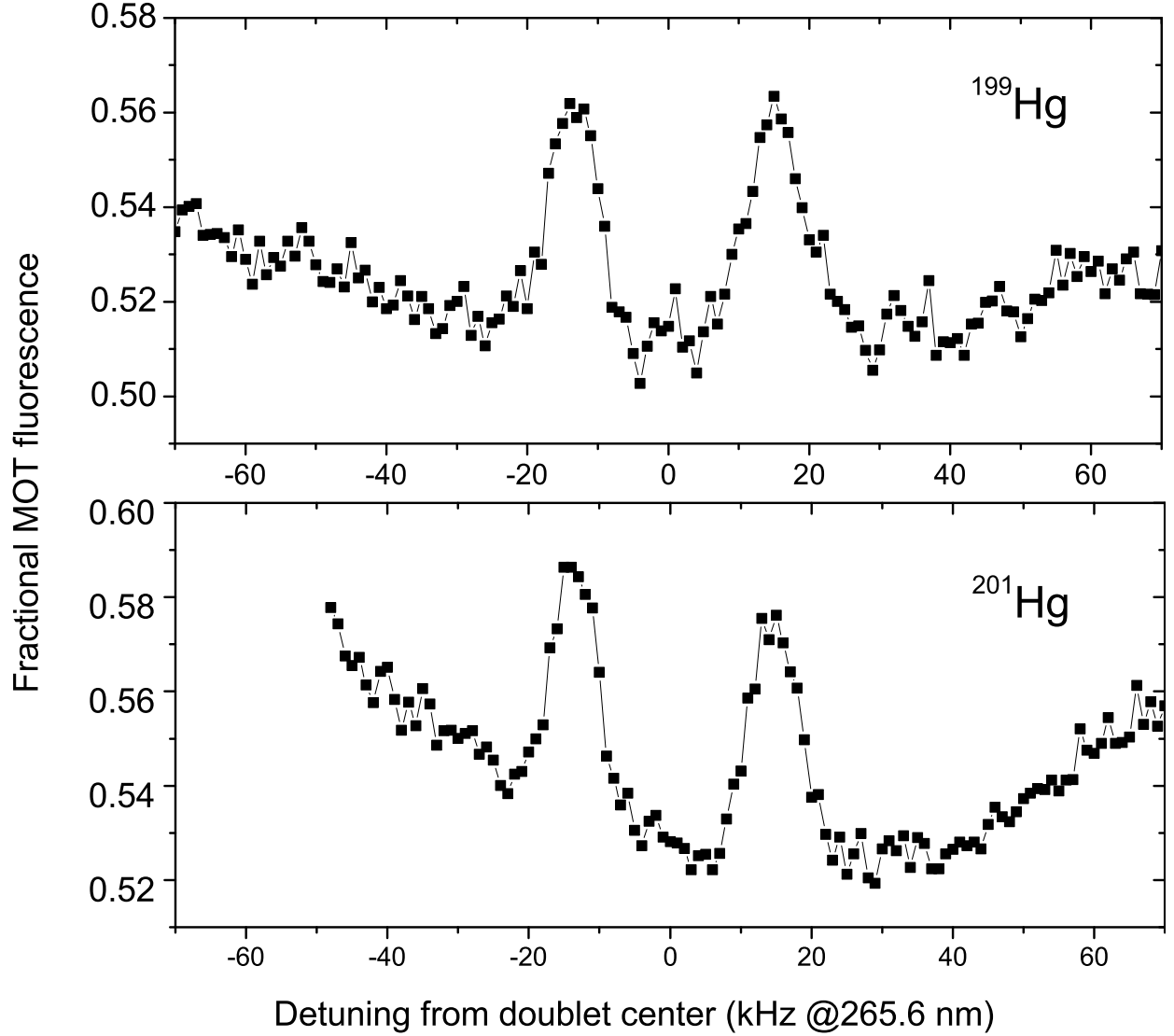


FIG. 4: Recoil doublet observed in the  $^{199}\text{Hg}$  (top) and  $^{201}\text{Hg}$  (bottom) spectra when a retro-reflected probe beam is used. Data are taken at a rate of one point per second. Spectra have been averaged 4 times.

the interaction time. Indeed, the maximum Rabi frequency that we estimate based on the probe beam power and size, and from the natural linewidth of the clock transition [17] is  $\sim 6$  kHz. It is smaller than the frequency chirp induced by the fall under the acceleration due to gravity  $g$  during the interaction time  $\tau$  which is  $g\tau/\lambda \simeq 18$  kHz for a typical value  $\tau = 500 \mu\text{s}$ . Note that the recoil doublet was also observed under similar conditions in  $^{40}\text{Ca}$  [23]. However, our  $^1S_0$ – $^3P_0$  mercury transition has a 3740 times narrower natural linewidth.

To determine the atomic transition frequency, we take the center of the recoil doublet. An



uncertainty equal to the half-width at half-maximum of the narrowest observed Doppler-free recoil feature is conservatively assigned to this determination. This amounts to a 4.5 kHz uncertainty for both  $^{199}\text{Hg}$  and  $^{201}\text{Hg}$ . When the MOT field is left on during the probe time, atoms at the edge of the cloud can be exposed to a field of up to 0.2 mT. With the MOT field off, the residual field due to unshielded magnetic sources is  $\sim 0.3$  mT. A worst case estimation of the shift induced by the first order Zeeman effect in such fields is 3.3 kHz for  $^{199}\text{Hg}$  and 2.8 kHz for  $^{201}\text{Hg}$ , given the nuclear magnetic moment and the magnetic moment difference between the two clock states [14]. Measurements performed with and without switching off the MOT field agree to within 700 Hz. A Stark shift of clock states due to the probe laser is less than 100 Hz. Finally, it is noteworthy that the overall standard deviation of all measurements is less than 1 kHz. The measured frequencies are  $\nu(^{199}\text{Hg}) = 1128575290808 \pm 5.6$  kHz for  $^{199}\text{Hg}$  and  $\nu(^{201}\text{Hg}) = 1128569561140 \pm 5.3$  kHz for  $^{201}\text{Hg}$ . In fractional terms, the uncertainty is  $\sim 5$  parts in  $10^{12}$  which improves previous indirect determinations [24, 25, 26] by more than 4 orders of magnitude. The isotope shift between the two fermionic isotopes is  $5729668 \pm 7.7$  kHz. The isotope shift between the best known bosonic isotope  $^{198}\text{Hg}$  [24] and  $^{199}\text{Hg}$  is  $\nu(^{198}\text{Hg}) - \nu(^{199}\text{Hg}) = 699 \pm 12$  MHz with an uncertainty dominated by the  $^{198}\text{Hg}$  uncertainty.

To summarize, we have reported the first laser-cooled spectroscopy of  $^1S_0$ – $^3P_0$  clock transition in fermionic isotopes of mercury. Owing to the observation of the Doppler-free recoil doublet, we have measured the transition frequency with an uncertainty which will make spectroscopy of the clock transition in a lattice trap straightforward. This is an important step towards producing a mercury lattice clock with unprecedented accuracy.

The authors would like to acknowledge support from SYRTE technical services. SYRTE is Unité Mixte de Recherche du CNRS (UMR CNRS 8630). SYRTE is associated with Université Pierre et Marie Curie. This work is partly funded by the cold atom network IFRAF. This work received partial support from CNES.

- 
- [1] T. Rosenband, et al., *Science* **319**, 1808 (2008).
  - [2] M. M. Boyd, et al., *Phys. Rev. Lett.* **98**, 083002 (2007).
  - [3] A. D. Ludlow, et al., *Science* **319**, 1805 (2008).

- [4] T. Schneider, E. Peik, and C. Tamm, Phys. Rev. Lett. **94**, 230801 (2005).
- [5] H. Marion, et al., Phys. Rev. Lett. **90**, 150801 (2003).
- [6] M. Fischer, et al., Phys. Rev. Lett. **92**, 230802 (2004).
- [7] S. Blatt, et al., Phys. Rev. Lett. **100**, 140801 (2008).
- [8] T. M. Fortier, et al., Phys. Rev. Lett. **98**, 070801 (2007).
- [9] E. Peik, et al., Phys. Rev. Lett. **93**, 170801 (2004).
- [10] N. Poli, et al., Phys. Rev. A **77**, 050501(R) (2008).
- [11] S. G. Porsev and A. Derevianko, Phys. Rev. A **74**, 020502(R) (pages 4) (2006).
- [12] (2004), V.G. Pal'chikov, private communication (2004) and H. Katori et al., in proc. of the XIX International Conference on Atomic Physics (2004).
- [13] M. Petersen, et al., in *Proc. of the 2007 EFTF-FCS joint meeting, Geneva, Switzerland* (2007).
- [14] H. Hachisu, et al., Phys. Rev. Lett. **100**, 053001 (2008).
- [15] E. J. Angstmann, V. A. Dzuba, and V. V. Flambaum, Phys. Rev. A **70**, 014102 (2004).
- [16] M. Petersen, et al., in *Proc. of the 2008 Frequency Control Symposium, Honolulu, USA and Proc. of the 2008 European Frequency and Time Forum, Toulouse, France* (2008).
- [17] M. Bigeon, Journal de Physique **28**, 51 (1967).
- [18] K. Dieckmann, R. J. C. Spreeuw, M. Weidemüller, and J. T. M. Walraven, Phys. Rev. A **58**, 3891 (1998).
- [19] D. Chambon, et al., Rev. Sci. Instrum. **76**, 094704 (2005).
- [20] I. Courtillot, et al., Phys. Rev. A **68**, 030501(R) (2003).
- [21] C. W. Hoyt, et al., Phys. Rev. Lett. **95**, 083003 (2005).
- [22] J. L. Hall, C. J. Bordé, and K. Uehara, Phys. Rev. Lett. **37**, 1339 (1976).
- [23] T. M. Fortier, et al., Phys. Rev. Lett. **97**, 163905 (2006).
- [24] E. B. Saloman, J. Phys. Chem. Ref. Data **35**, 1519 (2006).
- [25] K. Burns and K. B. Adams, J. Opt. Soc. Am. **42**, 716 (1952).
- [26] K. Burns and K. B. Adams, J. Opt. Soc. Am. **42**, 56 (1952).